Radiology

Elbow Imaging in Sport: Sports Imaging Series[1]

Matthew D. Bucknor, MD
Kathryn J. Stevens, MD
Lynne S. Steinbach, MD

Elbow pain is a frequent presenting symptom in athletes, particularly athletes who throw. The elbow can be injured as a result of acute trauma, such as a direct blow or a fall onto an outstretched hand or from chronic microtrauma. In particular, valgus extension overload during the throwing motion can precipitate a cascade of chronic injuries that can be debilitating for both casual and high-performance athletes. Prompt imaging evaluation facilitates accurate diagnosis and appropriate targeted interventions.

Online SA-CME
See www.rsna.org/education/search/ry

Learning Objectives:

After reading the article and taking the test, the reader will be able to:

- Discuss how CT, MR imaging, or US can be used to evaluate different pathologic conditions within the elbow
- Define the concept of valgus extension overload syndrome and its key imaging features
- Describe variant anatomy in the elbow, which may mimic disease in athletes who throw
- Discuss postoperative imaging features in athletes who undergo surgery for ulnar collateral ligament injury or ulnar neuritis
- Explain the imaging differences between various childhood elbow injuries
- Discuss the most common tendon and nerve injuries within the elbow and their associated findings

Accreditation and Designation Statement

The RSNA is accredited by the Accreditation Council for Continuing Medical Education (ACCME) to provide continuing medical education for physicians. The RSNA designates this journal-based SA-CME activity for a maximum of 1.0 *AMA PRA Category 1 Credit*™. Physicians should claim only the credit commensurate with the extent of their participation in the activity.

Disclosure Statement

The ACCME requires that the RSNA, as an accredited provider of CME, obtain signed disclosure statements from the authors, editors, and reviewers for this activity. For this journal-based CME activity, author disclosures are listed at the end of this article.

[1]From the Department of Radiology and Biomedical Imaging, University of California–San Francisco, 185 Berry St, Lobby 6, Suite 350, San Francisco, CA 94158. Received March 17, 2015; revision requested April 22; revision received September 22; accepted October 2; final version accepted November 2. **Address correspondence to** M.D.B. (e-mail: *matthew.bucknor@ucsf.edu*).

Elbow pain is a frequent presenting symptom in many athletes, particularly those participating in overhead throwing sports, because of the high valgus forces placed on the elbow in extension. Several sports in particular are commonly associated with elbow pain, including baseball, softball, football, tennis, golf, and javelin throwing. The incidence of elbow pain in baseball players, for example, is between 20%–30% for 8–12 year olds, approximately 45% for 13–14 year olds, and over 50% for high school, college, and professional athletes (1,2). Acute injuries often occur as a result of direct trauma or a fall onto the outstretched hand. Chronic repetitive microtrauma to joints and their supporting soft-tissue structures can result in debilitating pain that prevents return to activity.

Essentials

- MR imaging is the recommended imaging modality for establishing specific patterns of acute and chronic osseous and soft-tissue injuries of the elbow.
- Dynamic US is recommended for real-time guidance of injections of local anesthetic, steroids, or platelet-rich plasma around the ligaments and tendons of the elbow to facilitate healing and pain relief.
- Increased valgus force leads to injury of the ulnar collateral ligament and the broad spectrum of both ulnar- and radial-sided disease, which encompasses valgus extension overload syndrome.
- MR imaging is the most sensitive modality for diagnosing lateral epicondylosis, the most common cause of elbow pain, but US can be useful for guiding therapeutic procedures.
- Posterolateral rotatory instability, the most common chronic instability of the elbow, should be considered with the presence of radiocapitellar incongruity, ulnohumeral incongruity, or lateral ulnar collateral ligament injury on MR images.

Basic Anatomy

The elbow is a complex joint with three distinct bony articulations: the ulnohumeral (hinge), radiocapitellar (hinge and pivot), and radioulnar (pivot) joints, which are enveloped by a single synovial capsule. The ulnohumeral joint is the most important osseous stabilizer of the elbow, providing primary stability at less than 20° of flexion or greater than 120° of flexion (3,4). Even partial osseous resection, such as cheilectomy of posteromedial osteophytes along the olecranon, can significantly increase total varus/valgus laxity.

The ulnar collateral ligament (UCL) and radial collateral ligament complex are important soft-tissue stabilizers of the elbow (Figs 1, 2). The UCL is composed of three bundles: anterior, posterior, and transverse (5,6). The anterior bundle is the primary restraint to valgus stress at the elbow and is normally seen on two to three consecutive coronal images, demonstrating low signal intensity at both T1- and T2-weighted magnetic resonance (MR) sequences (Fig 3). Some regions of higher signal intensity can be seen normally at the attachment to the medial epicondyle secondary to fibrofatty slips (3,7). The posterior bundle has a fan-shaped configuration and arises more inferiorly from the medial epicondyle of the humerus, attaching to the posteromedial aspect of the trochlear notch of the ulna (4,6). The transverse bundle does not significantly contribute to joint stability (4,5,8).

The radial collateral ligament complex provides varus stability to the elbow and is composed of three main structures: the radial collateral ligament, the lateral UCL (LUCL), and the annular ligament. The annular ligament surrounds the head and neck of the radius, anchoring the proximal radius to the radial notch of the ulna. The radial collateral ligament arises from the lateral epicondyle of the humerus with its distal fibers blending into the annular ligament and radial neck. Finally, the LUCL arises from the lateral epicondyle of the humerus near the origin of the radial collateral ligament, just deep to the common extensor tendon origin. It courses along the posterolateral margin of the radius then crosses to attach to the supinator crest of the ulna. The LUCL is the only bone-to-bone attachment along the lateral joint. It provides the principal restraint to varus stress.

Mechanisms of Injury

All athletes are at risk for acute injuries as a result of direct trauma or a fall onto the outstretched hand. However, overhead throwing athletes in particular are predisposed to elbow ligamentous injury and joint degradation as a consequence of the enormous forces placed on these structures during the throwing motion. Baseball throwing, for example, generates substantial valgus and extension forces. Biomechanical testing has estimated valgus forces of 64 N·m during the late cocking and acceleration phases with compressive forces of 500 N in the radiocapitellar joint as the elbow moves from 110° to 20° of flexion at velocities which may reach 3000°/sec (7,9,10). Large valgus forces with rapid elbow extension result in *(a)* tensile stress along the medial compartment restraints (UCL, flexor-pronator mass, medial epicondyle apophysis, and ulnar nerve), *(b)* shear stress in the posterior compartment (olecranon tip and trochlea/olecranon fossa), and *(c)* compressive stress laterally (radiocapitellar joint) (4,11). Additionally, overuse can lead to varying degrees of tendon degeneration and disruption in all four muscular compartments. This constellation of mecha-

Published online
10.1148/radiol.2016150501 **Content code:** MK

Radiology 2016; 279:12–28

Abbreviations:
FS = fat saturated
LUCL = lateral UCL
OCD = osteochondritis dissecans
PLRI = posterolateral rotatory instability
UCL = ulnar collateral ligament

Conflicts of interest are listed at the end of this article.

Figure 1

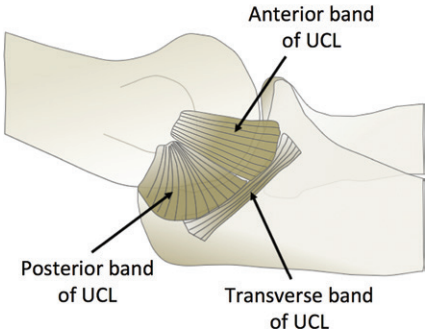

Figure 1: Diagram of the UCL complex on the medial elbow.

Figure 2

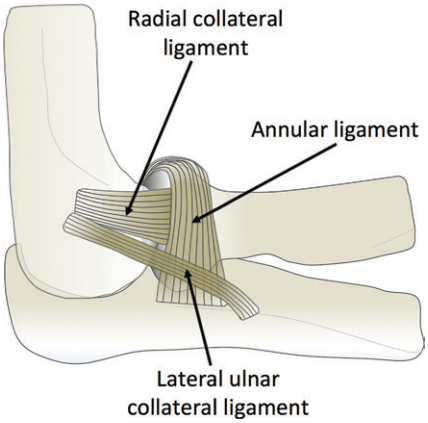

Figure 2: Diagram of the radial collateral ligament complex on the lateral elbow.

nisms composes the large fraction of sports injuries to the elbow.

Imaging Techniques

Radiography

Radiographs of the elbow are recommended to evaluate for possible fracture or dislocation following acute injury. Anteroposterior and lateral views are routinely obtained. Dedicated radial head and oblique views can also be obtained for more sensitive evaluation. Radiographs can also demonstrate the presence of a joint effusion after trauma, suggestive of an occult fracture. In the chronic setting, radiographs can also demonstrate soft-tissue calcification, ossification, osteophyte formation, or osteochondral defects, which may suggest tendon or ligament injury as a consequence of repetitive microtrauma. Stress views can be used to evaluate for ligamentous injury and stability but may be painful and are typically obtained in the operating room with fluoroscopy and general anesthesia.

Figure 3

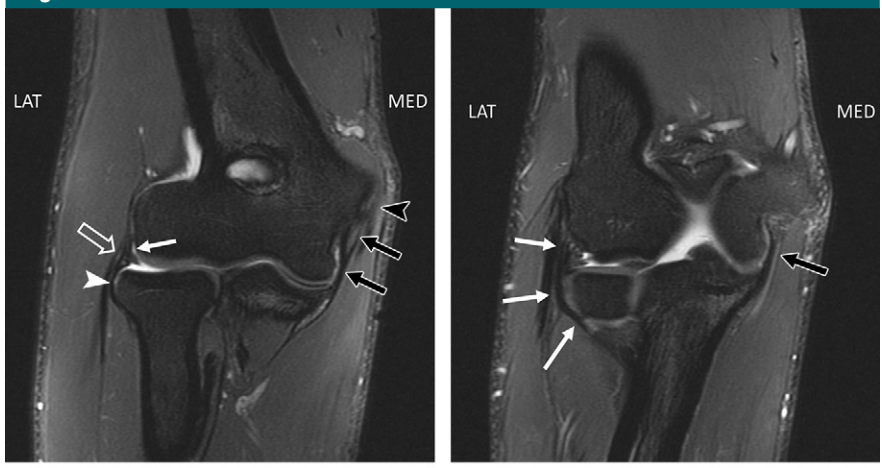

a. b.

Figure 3: **(a)** Coronal T2-weighted fat-saturated (FS) MR image through the elbow demonstrates the UCL (black arrows) and overlying common flexor tendon (black arrowhead) on the medial side *(MED)*. On the lateral side *(LAT)* is the radial collateral ligament with an adjacent synovial fold (white arrow), the annular ligament (white arrowhead), and the overlying extensor carpi radialis brevis origin (open arrow). **(b)** Coronal T2-weighted FS MR image through the elbow demonstrates the posterior band of the UCL (black arrow) on the medial side and LUCL (white arrows) on the lateral side.

Ultrasonography

Ultrasonography (US) offers a widely accessible, cost-effective technique for imaging the elbow and can be used to directly evaluate superficial soft-tissue injuries including ligament or tendon tears or neurovascular injuries (Fig 4) (12). High-resolution transducers, for example a 15-MHz linear array with a wide footprint or an 18-MHz linear array "hockey stick" transducer, provide high spatial resolution. Imaging can be tailored to evaluate a particular ligament or tendon of concern. Additionally, dynamic imaging can be performed—for example, in flexion/extension, supination/pronation, or under valgus/varus stress. Dynamic US is also an ideal method of image-guided intervention and can be used to provide real-time guidance of injections of local anesthetic, steroids, or platelet-rich plasma. US is less well suited for evaluation of osteochondral injuries and deep structures within the joint. An additional limitation is the dramatic variability in the image quality based on the operator. Furthermore, images obtained by one individual may be difficult for another clinician to interpret.

Computed Tomography

Computed tomography (CT) is frequently used in the acute setting to evaluate for fractures. It is particularly useful in demonstrating intraarticular extension of fractures, the distribution of small fracture fragments within and adjacent to the joint space, as well as any associated bony malalignment. For example, CT might best depict a "terrible triad" fracture-dislocation (radial head fracture, coronoid fracture, LUCL injury following dislocation), which might require surgery. Similarly, CT can precisely demonstrate the degree of displacement of an articular fracture (> 2 mm step-off or gap), which would indicate the need for internal fixation. On modern multidetector CT scanners, examinations take a few seconds, allowing for minimal patient discomfort with

Figure 4

Figure 4: Longitudinal US image in a 60-year-old man who fell off his bicycle and sustained a ruptured distal biceps tendon. The tendon end is retracted proximally (arrow) and surrounded by fluid.

high spatial resolution. Intravenous contrast material can be administered as an adjunct to examine for the presence of vascular injury or focal fluid collections. CT can also be useful in evaluating chronic pain following injury and can readily identify abnormal ossifications or calcifications which can be seen as a sequela of trauma, including osteochondral bodies, heterotopic ossification, or myositis ossificans. Intraarticular contrast material can be injected for improved visualization of joint bodies and cartilage. Osseous manifestations of secondary degenerative change are also well evaluated with CT. Less often, CT arthrography is performed for evaluation of ligamentous integrity in patients with contraindications to MR imaging.

MR Imaging

MR imaging is the reference standard for imaging evaluation of the supporting structures of the elbow, offering unparalleled soft-tissue contrast. Imaging is ideally performed at 3 T, which provides improved spatial resolution compared with examinations at 1.5 T, although this theoretical benefit is of unclear diagnostic value. Routine nonenhanced imaging provides comprehensive evaluation of the major ligaments, tendons, muscles, bones, and neurovascular bundles of the elbow. Routine nonenhanced imaging should consist of a mix of fat and fluid sensitive sequences. At our institutions, we typically perform the following sequences: coronal T1-weighted, coronal T2-weighted FS, axial T2-weighted FS, axial intermediate-weighted FS, sagittal T2-weighted FS, axial T1-weighted, and sagittal T1-weighted sequences (Table). All acquisitions are slightly oblique with respect to the joint line articulations. Intraarticular contrast material can be administered to improve sensitivity for detection of subtle partial tears of ligaments and joint bodies. The bony cortex is not as well evaluated at MR imaging compared with CT but the ability to detect subtle signal intensity changes in the marrow and periosteal soft tissues increases sensitivity to early stress changes in bone.

Patients can be imaged in either the prone or supine position. In the supine position, the patient's arm is positioned at his or her side. Patients are able to tolerate this positioning comfortably, resulting in minimal motion artifact, but because the elbow is not in the magnet's isocenter there can be significant field inhomogeneity, particularly on FS images. Short-tau inversion recovery (or STIR) imaging in this position provides more homogeneous fat suppression compared with frequency-selective techniques, albeit with a decreased signal-to-noise ratio (13). Conversely, imaging in the prone position places the elbow in the center of the magnet and allows for more uniform field homogeneity and fat saturation at the expense of patient comfort and increased motion artifact.

Arthrography

With modern imagers, nonenhanced MR imaging is usually sufficient to perform a comprehensive evaluation of the joint. However, arthrography can be used to distend the joint and potentially improve detection of subtle findings at both MR imaging and CT in certain patient populations. MR arthrography might be considered for a high-performance athlete for whom a diagnosis of a subtle partial tear of the UCL might indicate the need for reconstruction of that ligament (11,14,15). CT arthrography is useful for evaluation of the integrity of elbow ligaments and joint capsule in patients with contraindications to MR imaging. Both MR and CT arthrography are sensitive and specific for the diagnosis of early and advanced cartilage lesions (16).

CT arthrography has also been used to evaluate for the presence of intraarticular bodies. However, its utility in this capacity is unclear. One study suggested that neither CT arthrography nor MR imaging is significantly more accurate than radiography for the diagnosis of intraarticular bodies (17).

When arthrography is performed, the joint can be injected with a mixture of gadolinium, saline (or ropivacaine), and iodinated contrast material. With fluoroscopic guidance, the joint can be entered laterally over the radial head. Alternatively, a posterior approach has been suggested and is our preferred method to inject the elbow for an MR arthrogram to avoid the radial collateral ligament (18). Another approach to consider is the posterolateral approach between the olecranon, humerus, and radial head allowing the radial collateral ligament complex and triceps tendon to be avoided entirely in cases in which these structures might be under consideration for abnormality (19). Typically 3–6 mL is sufficient to adequately distend the joint. For MR arthrography, the following sequences are routinely performed: co-

MR Sequences Used for Evaluation of the Elbow

Sequence	Echo Time (msec)	No. of Echoes	Repetition Time (msec)	Echo Train Length	Section Thickness (mm)	Section Spacing (mm)
Nonenhanced MR imaging						
Coronal T1-weighted	18.0	1	524.0	3	2.5	0.5
Coronal T2-weighted FS	54.0	1	3457.0	10	2.5	0.5
Axial T2-weighted FS	54.0	1	3659.0	8	2.5	0.5
Axial intermediate-weighted FS	24.0	1	3333.0	7	2.5	0.5
Sagittal T2-weighted FS	54.0	1	3500.0	8	2.5	0.5
Axial T1-weighted	18.0	1	685.0	3	2.5	0.5
Sagittal T1-weighted	18.0	1	516.0	3	2.5	0.5
MR arthrography						
Coronal T-weighted	18.0	1	800.0	2	2.5	0.5
Coronal T2-weighted FS	54.0	1	4000.0	15	2.5	0.5
Axial T2-weighted FS	54.0	1	4000.0	15	3.0	1
Axial T1-weighted FS	18.0	1	800.0	3	2.5	0.5
Sagittal T2-weighted FS	54.0	1	4000.0	15	2.5	0.5
Sagittal T1-weighted FS	18.0	1	800.0	2	2.5	0.5

ronal T1-weighted, coronal T2-weighted FS, axial T2-weighted FS, axial T1-weighted FS, sagittal T2-weighted FS, and sagittal T1-weighted FS.

Choice of Modality

All four imaging modalities are versatile and capable of demonstrating abnormalities of bone, cartilage, ligaments, and tendons. We summarize a typical imaging schema used at our two institutions in Figure 5. Generally, radiographs are a recommended first-line modality following acute trauma to evaluate grossly for the presence of fracture or dislocation. US is the study of choice for evaluating a specific ligament or tendon and providing real-time guidance of injected therapy. CT is useful to more completely delineate acute bony injury and most accurately depict heterotopic ossification in patients with chronic injury, while CT arthrography can provide an assessment of capsular integrity in patients with contraindications to MR imaging. Finally, nonenhanced MR imaging is the routine reference standard for evaluation of soft-tissue abnormalities around the elbow in athletes. MR arthrography is most often indicated in high-performance athletes in whom the diagnosis of subtle capsular injuries might require surgical intervention.

Figure 5

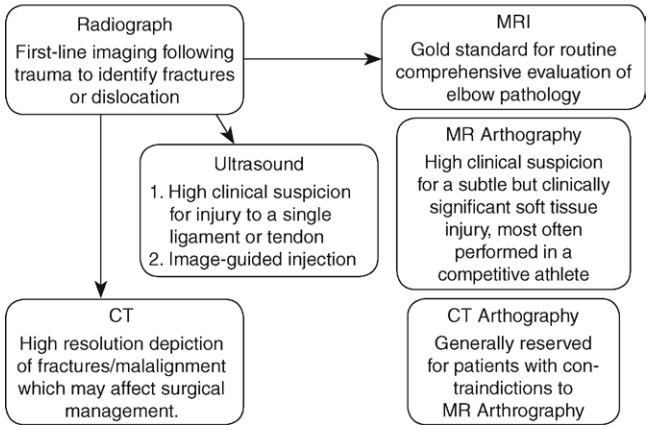

Figure 5: Diagram of the guidelines for the use of each modality.

Valgus Extension Overload Syndrome

Evaluation of the UCL is one of the leading indications for MR imaging evaluation of the elbow in the throwing athlete. UCL degradation or failure in the face of repeated stress precipitates more excessive valgus moments with resultant high tensile forces across the medial elbow (UCL, flexor-pronator mass, ulnar nerve), shear and impingement forces within the posterior compartment, and compressive forces across the lateral elbow (eg, the radiocapitellar joint) (3,4,8). Of note, pediatric throwing athletes develop unique pathologic conditions along the medial (medial epicondyle apophysitis) and lateral joint (osteochondritis dissecans [OCD] and osteochondrosis) as a consequence of repetitive valgus stress.

Ulnar Collateral Ligament

During elbow extension, high tensile forces on the ulnar side of the elbow from extreme valgus torques place considerable stress on the anterior bundle of the UCL. Injury can occur as a result of either direct valgus stress or repetitive valgus microtrauma (20). Most

Figure 6

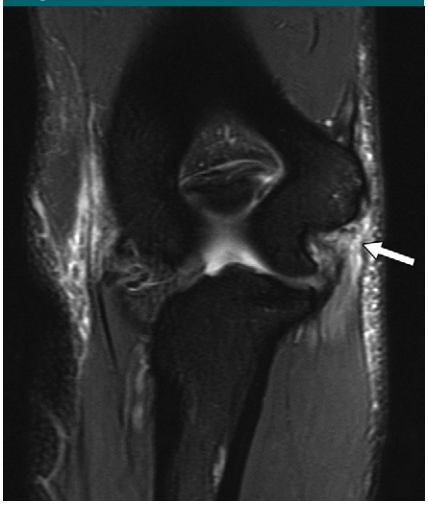

Figure 6: Coronal T2-weighted FS MR image in a 20-year-old male varsity gymnast with an acute hyperextension injury demonstrates a proximal tear of the medial collateral ligament (arrow). A decision was made to treat this injury nonoperatively.

Figure 7

Figure 7: Coronal T2-weighted FS MR image in a 21-year-old female water polo player 4 weeks after a valgus injury demonstrates thickening and increased signal intensity in the anterior band of the UCL (arrows), compatible with partial tearing and moderate grade sprain. Bone marrow edema is seen in the capitellum and radial head (*) from associated impaction injury. This injury was treated nonoperatively and is not surgically proven.

Figure 8

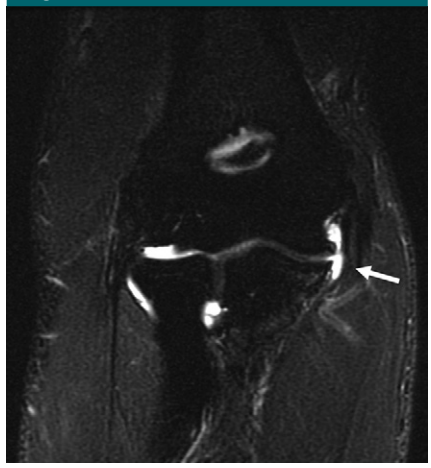

Figure 8: Coronal T2-weighted FS MR image in a 23-year-old man with acute elbow injury demonstrates a partial undersurface tear of the distal UCL, with fluid interposed between the distal UCL and sublime tubercle, forming the so-called T sign (arrow). This injury was treated nonoperatively and is not surgically proven.

tears occur within the midsubstance of the anterior bundle, although avulsions of either the proximal or distal attachment also occur (9,10,21). Low-grade sprains manifest as periligamentous edema with grossly intact fibers. In moderate and higher grade injuries, linear and complex regions of increased signal intensity traverse the fibers with adjacent edema-like changes.

Patients with complete UCL tears have substantial valgus instability at clinical examination. The imaging diagnosis of a complete or high-grade tear is also usually straightforward, with ligament discontinuity and abnormal fiber laxity (Fig 6). However, partial thickness tears are more variable in clinical and radiologic presentation. On MR images, they are most frequently seen as periligamentous edema-like change with varying degrees of increased signal intensity on T2-weighted images traversing the ligament fibers (Fig 7). Partial tears of the distal attachment at the sublime tubercle have a characteristic appearance secondary to fluid or contrast material insinuating below the ligament along the margin of the bone, commonly referred to as the "T sign" (Fig 8). However, the distal insertion can normally lie up to 3 mm distal to the articular cartilage, which can result in an appearance similar to the "T sign"—a potential diagnostic pitfall (11). Additionally, the normally tight connection between the anterior band of the UCL and the sublime tubercle is variable in older patients, in whom a slight distance can be present normally (3,22). In these scenarios, the presence of periligamentous edema is a useful secondary sign of the presence of a tear. Within the spectrum of partial tears, those of the proximal attachment have a more significant impact on posteromedial elbow biomechanics (21,23).

Variability in the imaging presentation of partial tears of the UCL can make this a challenging diagnosis on MR images. Schwartz et al (11) reported 92% sensitivity (24 of 26 patients) and 100% specificity (14 of 14 patients) for diagnosis of UCL tears with saline-enhanced MR arthrography (11,24,25). Sensitivity for complete tears was 95% (18 of 19 patients) compared with 86% (six of seven patients) for partial tears. In a study of CT arthrography and nonenhanced MR imaging with surgical confirmation, Timmerman et al (22) found that while both techniques were 100% sensitive for complete tears, nonenhanced MR imaging had an overall sensitivity of 57% (eight of 14 patients) and specificity of 100% compared with 86% (12 of 14 patients) and 91%, respectively, for CT arthrography (22).

The MR imaging appearance of the UCL is frequently abnormal in asymptomatic athletes who participate in overhead throwing sports. This can range from thickening to partial tearing. For example, in a retrospective study of 21 professional asymptomatic baseball pitchers, Del Grande et al (23) found that 48% (10 of 21) and 10% (two of 21) of the subjects showed partial tears of the anterior and posterior bundles of the UCL, respectively. Increased signal intensity that did not meet criteria for tear was seen in 43% (nine of 21) of the anterior UCLs, but none of the posterior UCLs (23,26,27). These results suggest that overhead throwing athletes experience chronic repetitive trauma to the UCL and many patients who progress to higher grade

tears likely have pre-existing abnormalities of the ligament.

While MR imaging facilitates a comprehensive evaluation in most cases, the anterior bundle of the UCL is also amenable to evaluation with dynamic US (24,25,28). The patient is typically positioned with the elbow in extension and the forearm fully supinated. The ligament is best seen in the coronal plane and normally appears as a predominantly hyperechoic structure with interspersed relatively hypoechoic collagen fibers (24,29). Tears are demonstrated as loss of the normal highly organized structure with associated regions of fluid and edema. At our institutions, we generally reserve the use of US for cases when our referring orthopedic surgeons need to assess the integrity of the ligament under valgus stress.

Postoperative Evaluation of the UCL

Surgical reconstruction of the UCL (also known as Tommy John surgery) is indicated in *(a)* throwing athletes with a complete UCL tear, *(b)* partial tears that have failed rehabilitation, and *(c)* symptomatic nonthrowing athletes after 3 months of rehabilitation (26,27,30). The procedure involves using a tendon graft to replace the function of the torn UCL. On MR images, a UCL reconstruction demonstrates increased intrasubstance signal intensity related to suture material and granulation tissue, which decreases with time (approximately 6 months) (28,31). Usually, the reconstructed ligament eventually demonstrates low signal intensity. However, Wear et al (29) demonstrated that approximately 24% of patients (12 of 51) continued to demonstrate intermediate signal intensity on T1- or T2-weighted images, particularly proximally (29,32). The graft can also appear thickened, in part related to the double bundle technique with suturing (as opposed to excision) of the native ligament, with a broad attachment proximally (Fig 9). This thickening should not be confused for an abnormality within the adjacent common flexor. While the graft may appear thickened, it should remain taut in appearance. Redundancy or waviness suggests possible partial tearing. Additionally, because the distal graft tunnels in the ulna are approximately 3–4 mm distal to the articular surface, an apparent T-sign distally often reflects the normal graft insertion and should not be mistaken for a partial tear.

Complications of UCL reconstruction are reported to be less than 10% (33). Radiographs should be evaluated for the presence of abnormal valgus alignment and hardware loosening or failure. On MR images, the graft should be assessed for tears, redundancy, or excessive scar tissue. MR arthrography has increased sensitivity for partial tears in the postoperative setting. The ulnar nerve can be injured following UCL reconstruction secondary to laceration or compression. It is also frequently decompressed in association with UCL reconstruction. The course, caliber, and signal intensity of the ulnar nerve should be carefully evaluated to the levels above and below the reconstruction. In addition to interval soft-tissue injury, Schwartz et al (30) described avulsion of the medial epicondyle as a rare complication of UCL reconstruction in seven throwing athletes, involving the humeral tunnel or tunnels of the UCL reconstruction, which can act as a stress riser (30,34). The diagnosis can typically be readily made by means of radiography, CT, or MR imaging.

Posteromedial Impingement

Within the posterior compartment, excessive shear forces can result in osteophytes at the posteromedial tip of the olecranon, with a corresponding "kissing lesion" within the olecranon fossa and posteromedial trochlea, and associated synovitis. This constellation of findings is referred to as posteromedial impingement. The development of osteophytes further exacerbates the degree of impingement, leading to a self-perpetuating cycle of degenerative changes. Radiography can be useful in demonstrating osteophyte formation. As degeneration and valgus stress progresses, osteophytes can fracture and distribute within the joint space, leading to mechanical symptoms (31). Patients typically complain of pain during extension or follow-through (31,32). In adults, these shear forces can also result in characteristic oblique fractures through the olecranon (34,35).

Nonenhanced MR imaging can be used to identify the size and location of associated intra-articular bodies along with chondrosis, subchondral sclerosis, cystic change, and edema (Fig 10). CT and MR arthrography can increase sensitivity for detection of joint bodies. In a small retrospective study of nine throwing athletes, Cohen et al (31) found a reproducible pattern on MR images in patients with clinical diagnoses of posteromedial impingement (4,31). All patients had degenerative changes at the articular surfaces of the posterior trochlea and the anteromedial olecranon including cartilage signal heterogeneity, focal cartilage defects, and subchondral bone marrow edema, in addition to synovitis within the posteromedial recess. Edema about the distal medial triceps was also a frequent finding seen in eight of nine patients (31,36). In another study by Kooima et al (35), 13 of 16 asymptomatic professional baseball players demonstrated similar findings consistent with posteromedial impingement (35,37). The authors also found a significant correlation between UCL thickening and posteromedial subchondral sclerosis.

Figure 9

Figure 9: Coronal T1-weighted MR arthrographic image in a 22-year-old female gymnast with prior UCL reconstruction demonstrates an intact graft (arrows).

Figure 10

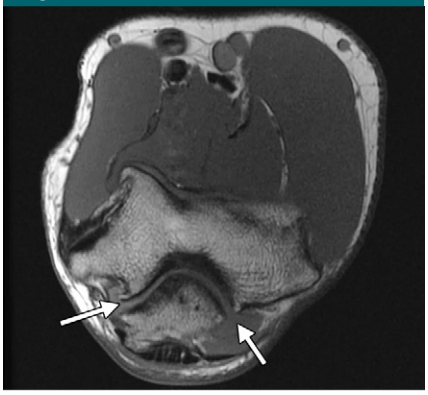

a.

b.

Figure 10: **(a)** Axial T1-weighted MR image in a 19-year-old baseball pitcher demonstrates subchondral sclerosis and osteophytosis in the posteromedial and posterolateral humeroulnar joint (arrows) compatible with valgus extension overload syndrome. **(b)** Sagittal T2-weighted FS MR image demonstrates two joint bodies in the olecranon fossa (arrowheads). Subsequent surgery confirmed the presence of posteromedial arthritis and multiple joint bodies.

Flexor-Pronator Mass Injuries

The common flexor-pronator tendon origin from the medial epicondyle provides important dynamic resistance to valgus stress in throwing athletes, particularly during early arm acceleration (4,38). Additional strain is placed on this muscle group during resisted flexion, for example during ball release (36,39). Athletes may develop a spectrum of abnormalities, including chronic tendinosis or medial epicondylosis (commonly referred to as medial epicondylitis or golfer's elbow), muscular overuse, and acute muscle or tendon tears. Avulsion from the medial epicondyle is more common than avulsion of the extensor group, even though epicondylosis is more common on the lateral side. Chronic symptoms are most likely related to incomplete healing of an avulsion injury to the common flexor tendon. As many as 60% of patients will have associated ulnar neuropathy at physical examination, in contrast to patients with common extensor tendon overuse symptoms, who rarely have associated radial nerve irritation (40).

Figure 11

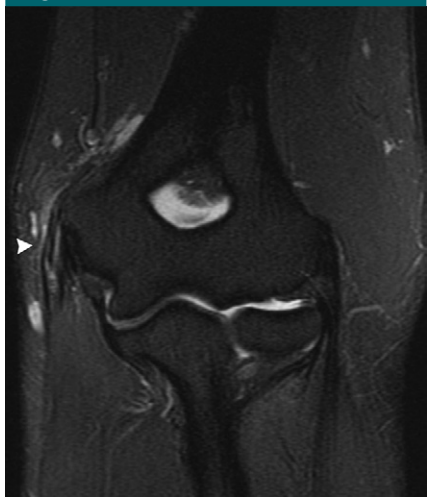

Figure 11: Coronal T2-weighted FS MR image in a 42-year-old man with medial epicondylosis demonstrates linear high T2 signal intensity in the common flexor tendon (arrowhead), with edema in the adjacent soft tissues.

MR imaging is useful in the evaluation of patients with flexor-pronator mass injuries, as symptoms overlap significantly with UCL tears and ulnar neuritis. In addition, UCL tears are commonly associated with injuries to the overlying flexor-pronator mass. The common flexor tendon is normally a low-signal-intensity structure on T1- and T2-weighted images arising from the medial epicondyle, well depicted on coronal images. In medial epicondylosis, the common flexor tendon appears thickened with increased intermediate signal intensity. Higher grade injuries manifest as fluid signal intensity traversing the tendon with adjacent peritendinous edema (Fig 11). The flexor carpi radialis and pronator teres tend to be the most severely affected components.

Medial Epicondyle Apophysitis

In the skeletally immature athlete, repeated valgus stress and/or repetitive forceful flexor-pronator muscle contraction can result in a fracture of the medial epicondyle apophysis. This injury is commonly seen in young baseball players and can progress to fragmentation and displacement of the apophysis. Bone marrow edema is seen within the apophysis on T2-weighted MR images and precedes radiographic findings (Fig 12). On radiographs, more advanced disease manifests as fragmentation or separation of the apophysis. Hang et al (37), in a study of 343 Little League baseball players participating in regional and national championships, found that on radiographic evaluation, 57% (195 of 343) of the athletes had evidence of displacement of the medial apophysis compared with the contralateral nonthrowing arm (37,41,42). Of those, 19% (66 of 343) had evidence of fragmentation of the apophysis.

Ulnar Neuritis

Ulnar neuropathy is the most common peripheral neuropathy about the elbow. The ulnar nerve is exposed to high traction forces from valgus stress, which can increase with UCL injury in the setting of valgus extension overload. The nerve is also vulnerable to compression from osteophytes and flexor-pronator muscle hypertrophy, direct trauma, and friction. The nerve is most frequently affected within the cubital tunnel but can also be commonly compressed at the arcade of Struthers, medial intramuscular septum, medial epicondyle, within a hypertrophied medial head of the triceps muscle, and along the deep flexor-pronator aponeurosis. The floor of the cubital tunnel is formed by the posterior bundle of the UCL and the joint capsule. The roof is composed of the cubital tunnel retinaculum proximally (Osborne ligament) and the aponeurosis of the flexor carpi ulnaris (arcuate ligament) distally—the latter is

Figure 12

a. b.

Figure 12: **(a)** Coronal T2-weighted FS MR image of the elbow in a 14-year-old male baseball pitcher demonstrates bone marrow edema around the medial apophysis (arrow), compatible with "Little Leaguer" elbow. **(b)** Anteroposterior radiograph demonstrates subtle widening of the apophysis superiorly (arrow) with minimal adjacent sclerosis.

Figure 13

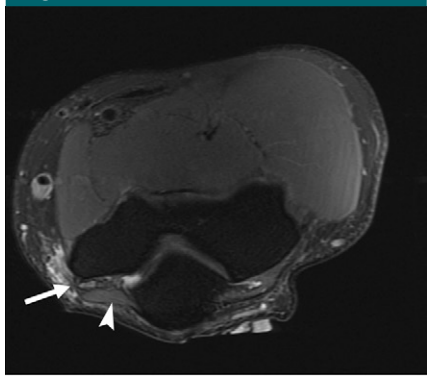

a.

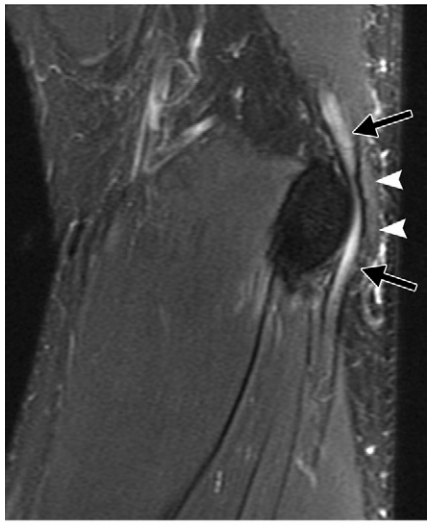

b.

Figure 13: **(a)** Axial intermediate-weighted FS and **(b)** sagittal T2-weighted FS MR images in a 32-year-old man with symptoms of ulnar neuritis demonstrate an accessory anconeus epitrochlearis (arrowheads) compressing the ulnar nerve (white arrow) in the cubital tunnel, with high signal intensity in the ulnar nerve proximal and distal to the tunnel (black arrows).

absent in up to 23% of subjects (38,39). When the elbow is flexed, the retinaculum becomes taut, compressing the nerve.

Variant anatomy can predispose athletes to ulnar neuritis (39,43). An anconeus epitrochlearis is a small anomalous muscle present in 23% of the population. Twenty-two percent of the population has a thickened cubital tunnel retinaculum (41,42,44). A low-lying medial head of the triceps muscle can also compress the ulnar nerve in the cubital tunnel (45). Variants also predispose certain patients to abnormal subluxation of the ulnar nerve over the medial epicondyle during flexion. For example, in 10% of the population, the cubital tunnel retinaculum is absent (46).

At MR imaging, the course of the ulnar nerve should be followed carefully on axial images. Findings can be subtle, and high-spatial-resolution MR neurography sequences with longer echo times can be used to increase the conspicuity of the findings (43,47). In patients with ulnar neuritis there can be focal or diffuse swelling of the nerve with obliteration of the normal cuff of fat. Ulnar nerve cross-sectional area can be useful for suggesting neuropathy, with one recent article demonstrating an area of 0.08 cm^2 as a cutoff that yielded 95% sensitivity and 80% specificity for the diagnosis of ulnar neuropathy (43). US can also be used to evaluate changes in nerve caliber and for the presence of nerve subluxation with flexion.

Diagnosis of ulnar neuropathy solely on the basis of abnormal nerve signal can be very difficult.

The ulnar nerve normally demonstrates mild intrinsic hyperintensity in many asymptomatic individuals because of endoneurial fluid but the nerve becomes somewhat more hyperintense in the setting of neuritis (39,48) (Fig 13). Relatively increased signal intensity of the nerve is sensitive but not specific for the presence of ulnar neuropathy and is best recognized by comparison to the more proximal or distal course of the nerve. Signal intensity changes on short-tau inversion recovery images are more accurate for the presence of neuropathy than frequency selective fat-suppressed images (43).

Postoperative Evaluation of the Ulnar Nerve

For patients with a compressive etiology, surgery is indicated in those with muscle weakness, fixed sensory loss, or significant denervation at electromyography (44,49). Surgical options include decompression with or without transposition. In simple decompression, as described by Osborne, the nerve is dissected and the cubital tunnel retinaculum or arcuate ligament is released with widening of the entrance between the two heads of the flexor carpi ulnaris muscle (48,50). In anterior transposition, the nerve is mobilized into the volar soft tissues: subcutaneous, submuscular, or intramuscu-

Figure 14

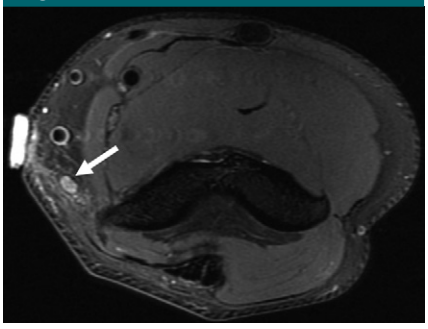

Figure 14: Axial intermediate-weighted FS MR image in an 18-year-old male water polo player, who had recurrent symptoms of ulnar neuritis following anterior transposition of the ulnar nerve, including pain, numbness, and tingling in his fourth and fifth digits. Increased signal intensity is seen within the transposed ulnar nerve (arrow). At electromyography there was decreased recruitment and isolated denervation of the flexor digitorum profundus, first dorsal interosseous, and abductor digiti minimi muscles, consistent with acute ulnar neuropathy. Subsequent surgery found scarring in both the ligament of Struthers and the fascial sling, and the patient's symptoms abated after the transposed nerve was released.

Figure 15

Figure 15: **(a)** Axial T2-weighted FS and **(b)** sagittal intermediate-weighted MR images in a 15-year-old male baseball player with elbow pain and a surgically proven 14-mm osteochondral lesion (arrow) in the capitellum (seen on 1.5-T images). Images show the round lesion with surrounding bone marrow edema-like changes and overlying cartilage loss. **(c)** Coronal and **(d)** sagittal T2-weighted images of the elbow in a 53-year-old woman with lateral epicondylosis. Images demonstrate subcortical cystic change (arrow) along the posterior portion of the capitellum, compatible with a pseudodefect, not to be mistaken for an osteochondral lesion.

lar. Fixed structural abnormalities or hypermobility of the nerve are considered indications for transposition, although the complication rate has been reported to be higher with anterior transposition (47,51). On MR images, the course, caliber, and signal intensity of the nerve at the level of the decompression should appear similar to the region of the nerve above or below the region of surgery (Fig 14). The muscles innervated by the nerve should also be evaluated for evidence of denervation.

Lateral Radiocapitellar Compression

The lateral radiocapitellar joint is normally responsible for approximately 30% of the restraint to valgus stress (49,52). As with posteromedial impingement, once the UCL is injured, increasing loads are placed on the lateral joint. On occasion, patients with UCL injuries present primarily with lateral symptoms, due to "kissing contusions" in the radiocapitellar joint (Fig 7). Continued valgus stress leads to repetitive lateral compression, resulting in chondromalacia, osteophyte formation, and loose bodies (50,53). Lateral radiocapitellar compression typically follows the development of posteromedial impingement. MR imaging is the study of choice for evaluation of chondral degeneration and loose bodies.

OCD is a focal osteochondral lesion of the lateral elbow, most frequently involving the capitellum, although the radial head can also be affected. It is typically seen in younger skeletally immature athletes, aged 10 to 15 years, particularly throwing athletes and gymnasts. While the exact etiology is unknown, a leading hypothesis is that lateral radiocapitellar compression results in vascular insufficiency along the subchondral plate, leading to bone death and microfracture. Routine radiography of the elbow has limited sensitivity for detecting the presence of an OCD lesion. Patients complaining of activity-related pain and stiffness or mechanical symptoms suggestive of OCD are best evaluated with MR imaging (51,54). MR imaging findings include a rim of low signal intensity on T1-weighted images with variable central signal intensity (Fig 15a, 15b). Unstable lesions dem-

onstrate a peripheral ring of increased signal intensity on T2-weighted images, or underlying cystic change, and are best seen with MR arthrography. Stable lesions more often demonstrate peripheral low signal intensity on T2-weighted images that blends with the normal adjacent bone marrow signal intensity (2,52). CT arthrography has similar accuracy compared with MR arthrography (16). Surgery is indicated for unstable lesions and stable lesions that do not respond to conservative management. One common pitfall in diagnosing an osteochondral injury is the pseudodefect of the capitellum, a normal bare area of bone along the lateral epicondyle which forms a sharp transition with the articular cartilage along the posteroinferior aspect of the capitellum (Fig 15c, 15d) (28,53).

A distinct condition frequently confused with OCD is osteochondrosis of the capitellum, also known as Panner disease, which typically affects boys less than 10 years of age. Boys may be more affected than girls because of the delayed maturation of their secondary ossification centers compared with girls. Similar to OCD, Panner disease is also believed to be a consequence of abnormally high valgus compressive forces along the radiocapitellar joint (54–56). However, current leading theory suggests that it is damage to the posterior-based end-arterial supply to the capitellum during a vulnerable period of endochondral ossification which results in the histologic and radiographic features similar to Legg-Calvé-Perthes disease in patients with Panner disease (2,57). Radiographs typically first demonstrate demineralization of the capitellum with poorly defined cortical margins. There is often associated sclerosis and fragmentation of the capitellar epiphysis (Fig 16). MR imaging demonstrates low signal intensity on T1-weighted images and high signal intensity on T2-weighted images throughout the capitellar ossification center (28,58). The natural history of Panner disease is characterized by symptom resolution after a period of immobilization.

While OCD and Panner disease may represent different parts of the spectrum of valgus stress abnormalities along the radiocapitellar joint, the differences in treatment and functional outcome make diagnostic distinction useful. In summary, age and sex can be very helpful in distinguishing between these two diagnoses, with Panner disease typically occurring in young boys less than 10 years of age and OCD occurring in patients 10–15 years of age. On MR images, OCD is more often marginated by a discrete rim of linear abnormal signal intensity and Panner disease more often demonstrates fragmentation and sclerosis.

Figure 16

a. b.

Figure 16: **(a)** Anteroposterior radiograph in a 7-year-old male patient with pain and decreased motion of the elbow demonstrates subtle sclerosis, subchondral lucency, and cortical irregularity of the capitellum (arrow), compatible with osteochondritis of the capitellum or Panner disease. **(b)** Corresponding coronal T1-weighted image shows irregular low signal intensity in the capitellum (arrow).

Other Tendon Disease

Lateral Epicondylosis

Lateral epicondylosis (also referred to as lateral epicondylitis or tennis elbow) is the most common cause of elbow pain and is frequently seen in athletes who throw, most commonly adults over 35 years of age (59,60). Repetitive loading of the extensor musculature results in a cycle of progressive overuse microtears with subsequent angiofibroblastic hyperplasia within the tendon substance (55–57,61,62). Inflammatory cells are usually not present. Less frequently, patients can develop symptoms from direct trauma to the tendon.

Clinical history and physical examination are often sufficient for diagnosis. However, MR imaging can be useful in patients who do not respond to conservative measures, allowing for quantification of the extent of tendon injury and assisting in preoperative planning. At MR imaging, the common extensor tendon is normally a vertically oriented band of low signal intensity on T1- and T2-weighted images that arises from the lateral epicondyle, just superficial to the radial collateral ligament complex. In patients with lateral epicondylosis, the tendon appears thickened, with increased intermediate signal intensity on T1- and T2-weighted images and varying degrees of adjacent reactive edema (Fig 17). Partial tears can be identified by fluid traversing tendon fibers or extensive edema surrounding tendon fibers, most frequently within the extensor carpi radialis brevis tendon. The LUCL can also be involved in patients

Figure 17

Figure 17: Coronal T2-weighted FS MR image in a 43-year-old man with a 1-year history of lateral elbow pain demonstrates increased T2-weighted signal intensity in the common extensor tendon (arrow), compatible with lateral epicondylosis. A mildly thickened and irregular plica is also seen in the radiocapitellar joint posterolaterally (arrowhead). The patient was treated nonoperatively.

Figure 18

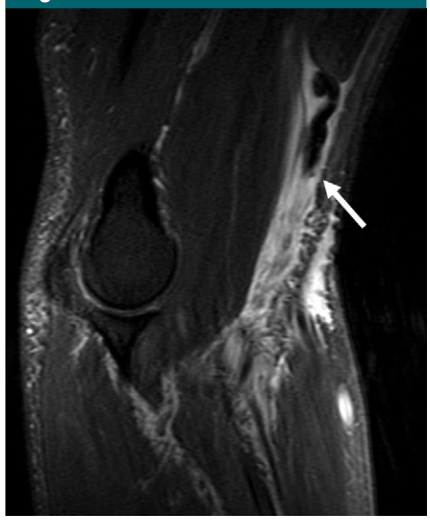

Figure 18: Sagittal T2-weighted FS MR image in a 48-year-old man with an acute injury lifting weights depicts avulsion of the distal biceps tendon with the tendon end retracted proximally (arrow).

with more severe disease and patients with lateral epicondylosis should be carefully evaluated for LUCL tears. Isolated surgical repair of the common extensor tendon in patients who also have a tear of the LUCL can destabilize the joint, resulting in posterolateral rotatory elbow instability. US can also be used to evaluate the common extensor tendon and guide percutaneous therapy, although it is less sensitive (64%–88%) than MR imaging (90%–100%) for detection of epicondylosis (58,63,64).

Biceps Tendon Disease

The distal biceps brachii tendon courses through the antecubital fossa to insert on the bicipital tuberosity of the radius. Superficial fibers forming the bicipital aponeurosis (or lacertus fibrosis) sweep medially from the distal tendon to anchor it to the fascia of the flexor-pronator mass. Distal biceps rupture is seen most frequently in weightlifters, particularly those using anabolic steroids. It is an uncommon injury in athletes, but may be seen, for example, in football players who experience forced extension of a flexed elbow. Clinically, avulsion often presents with a palpable mass in the upper arm secondary to retraction of the myotendinous junction. However, if the bicipital aponeurosis is not torn, the myotendinous junction retracts minimally and a complete avulsion from the tuberosity can be difficult to discern from a partial tear. MR imaging is useful in these situations to demonstrate the complete discontinuity of fibers in the setting of avulsion. The biceps tendon is best evaluated on sagittal and axial images. An appropriate field of view should be chosen so that the retracted tendon is not excluded from the images. Additionally, a FABS position (flexion, abduction, and supination) can be used as an adjunct to more completely visualize the distal insertion. If the bicipital aponeurosis is disrupted as well, there will be prominent proximal retraction of the myotendinous junction (Fig 18). Lower grade partial tears demonstrate intrasubstance and peritendinous increased signal intensity on T2-weighted images.

Chronic repetitive trauma can result in tendinopathy, manifesting as intermediate signal intensity within the tendon, and there may be associated partial tearing. Proliferative enthesopathy may develop in the radial tuberosity. These can increase the risk of bicipital avulsion if there is superimposed acute trauma. The biceps does not have a distal tendon sheath but the bicipitoradial bursa along the posterior aspect of the distal biceps tendon and the interosseous bursa between the biceps tendon and the ulna can distend in response to repetitive injury, leading to bursitis.

US can be used to detect focal abnormalities within the tendon suggestive of tendinosis, in addition to partial tears, complete tears, and any associated fluid collections. The tendon can be evaluated from an antecubital, lateral, or medial approach. Anisotropy of the distal insertion with the anterior approach is improved by use of the lateral or medial approach (61,65).

Triceps Tendon Disease

The distal heads of the triceps converge to insert together onto the olecranon. The medial head tendon fibers insert slightly anterior and deep to the common tendon of the lateral and long heads and in some patients this separation is more discrete. For example, Athwal et al (62) found a separate medial head insertion in 53% (eight of 15) of cadaver specimens, compared with 47% of specimens in which the long, lateral, and medial heads inserted together (62,66). If low lying, this separate insertion can be associated with ulnar neuritis and snapping triceps syndrome (67). Triceps tendon ruptures are uncommon. The most frequent mechanism is a fall onto an outstretched hand, although they also occur in weightlifters and athletes involved in high-impact contact sports. Risk factors include anabolic steroids, corticosteroids, olecranon bursitis, and inflammatory arthritis (63,64,68). Complete rupture most commonly occurs at the olecranon. In some instances there are associated small cortical avulsion fractures of the olecranon or radial head fractures. Similar to evaluation of the biceps, both MR imaging and US can be used to discriminate complete from partial tears and help identify the location of retracted fibers (Fig 19). Of note, the medial head can avulse and retract sep-

Figure 19

Figure 19: Sagittal T2-weighted FS MR image of the elbow in a jiu jitsu fighter after a direct blow to the arm demonstrates avulsion of the distal triceps tendon (white arrow), with extensive overlying olecranon bursitis (black arrows). There is cortical disruption (arrowhead) compatible with a small osseous avulsion.

arately from the common tendon of the lateral and long heads (28,65).

Instability and Dislocation

Posterolateral Rotatory Instability

Posterolateral rotatory instability (PLRI) is the most common type of symptomatic chronic instability of the elbow. It occurs when the radius and ulna rotate externally relative to the distal humerus, resulting in posterior displacement of the radial head with respect to the capitellum, while the radioulnar joint remains intact. This differs from isolated dislocation of the radial head, in which the proximal radioulnar joint is disrupted while the ulnohumeral articulation remains intact (66,69,70). PLRI is the only mechanism that can result in elbow dislocation without a fracture.

PLRI occurs as a result of axial compression, valgus force, and torsion (supination) force at the elbow, classically as a result of a fall on an outstretched hand. This pattern of forces results in a specific pattern of ligamentous and osseous disruption extending from lateral to medial, known as the circle of Horii (68,71). In stage 1, the LUCL is disrupted in isolation, resulting in rotation and subluxation of the radial head. With additional injury, disruption then extends to involve the anterior and posterior joint capsule, along with the radial collateral ligament complex (stage 2), the posterior band of the UCL (stage 3A), and the anterior band of the UCL (stage 3B). These subsequent stages are associated with progressive subluxation of the radial head, perching of the coronoid process under the trochlea, and finally frank dislocation (28).

The MR imaging evaluation of PLRI requires careful evaluation of the elbow ligaments and capsule, particularly the LUCL, which is best seen on coronal images (Fig 20). Of note, on nonarthrographic images, the LUCL is completely visible in approximately 80% of patients and only partially visible over its entire course in 18% of patients (72). Thickening or attenuation can be seen in the setting of acute or chronic injury. Fluid signal within the substance of the ligament constitutes a partial tear and complete discontinuity is consistent with a full-thickness tear. Failure of the LUCL appears to occur most frequently at the humeral attachment (69,70,73). Associated subluxation of the radial head posterolateral to the capitellum is best appreciated on sagittal images (Fig 20). Posterolateral translation of the radial head of more than 1.2 mm (sensitivity 67%, specificity 70%) and axial ulnohumeral incongruity of more than 0.7 mm (sensitivity 63%, specificity 70%) are cutoffs that can be used as screening tools to aid the diagnosis of elbow instability (74).

Fracture-Dislocation

Complex instability refers to an injury that destabilizes the elbow because of osseous and ligamentous disruption (71,75). Two basic patterns of complex dislocations are seen in the elbow: *(a)* dislocation with ligament injury and radial head fracture and *(b)* dislocation with ligament injury and a combination of radial head and coronoid fractures, often referred to as the "terrible triad" (28,76). The former is associated with disruption of the UCL, radial collateral ligament, and/or annular ligament. The latter, more severe, injury is seen frequently in young, active patients and carries a significant risk of recurrent instability, stiffness, heterotopic ossification, and posttraumatic arthritis. Optimal management requires fixation of the radial head and coronoid fractures and reconstruction of the radial collateral ligament complex (73,77). CT is useful in demonstrating the size of the coronoid fracture in these patients: Small fractures do not necessarily require fixation but larger fractures that might lead to instability need to be fixed.

Similarly, more extensive radial head injuries which cannot be completely reduced might indicate the need for radial head replacement in lieu of fixation. MR imaging allows for evaluation of the complete pattern of osseous and ligamentous injury, facilitating any necessary surgical intervention.

Fracture

Athletes can also experience fractures in isolation secondary to a direct blow or repetitive stress. Several patterns of bony stress injuries are recognized in the elbow. Olecranon stress changes are well described in athletes who throw, and they can occur as a result of repetitive abutment of the olecranon into the olecranon fossa, traction from triceps activity during the deceleration phase of throwing, or impaction of the medial olecranon onto the medial wall of the olecranon fossa from valgus forces (75,78). Fractures of the olecranon can be divided into transverse and oblique patterns. The transverse type occurs predominantly from triceps traction and extension forces and the oblique pattern occurs predominantly secondary to valgus and extension forces (Fig 21). UCL insufficiency leads to increased valgus forces and is seen in association with the oblique type (76,79). In addition to olecranon stress fractures, a medial supracondylar stress fracture has also been described in late adolescent pitchers (78). This injury is most likely related to the combination

Figure 20

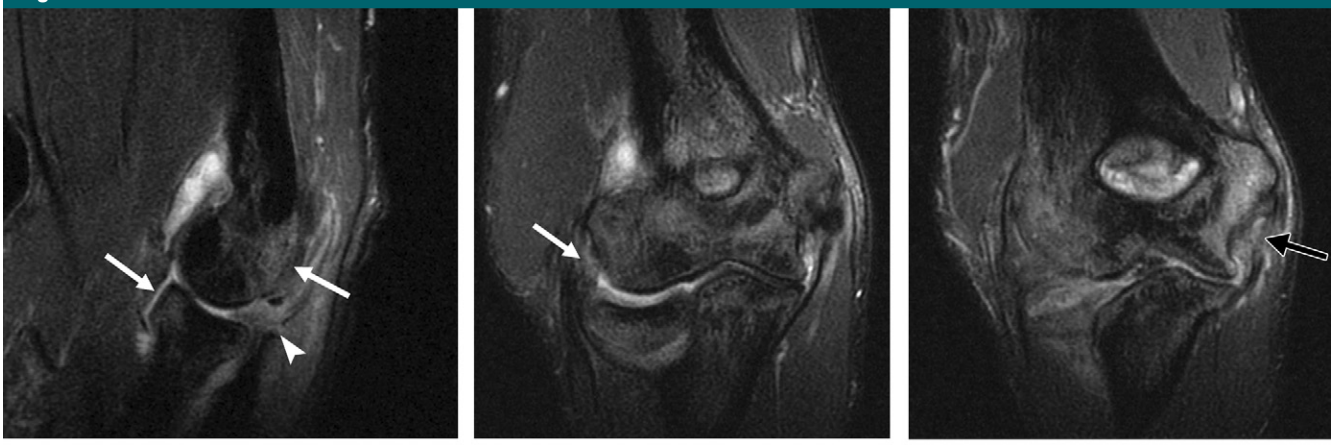

a. b. c.

Figure 20: **(a)** Sagittal T2-weighted FS MR image of the elbow in a 21-year-old man with recent posterior dislocation demonstrates characteristic "kissing contusions" on the posterior capitellum and anterior radial head (arrows) and disruption of the posterior joint capsule (arrowhead). There is also posterior subluxation of the radial head indicating a LUCL injury. **(b, c)** Coronal T2-weighted FS MR images show complete tears of the proximal LUCL (white arrow) and midfibers of the anterior band of the MCL (black arrow), with diffuse bone marrow edema.

of olecranon impingement and medial tension stress. While fractures can usually be seen at MR imaging, CT, or radiography, MR imaging is the most sensitive to subtle fracture lines and the presence of stress changes which often precede fracture (77,80). However, CT is useful in measuring the precise degree of displacement: Generally patients with more than 2 mm step-off or gap may require surgical fixation for fractures of the radial head, olecranon, or humerus.

Figure 21

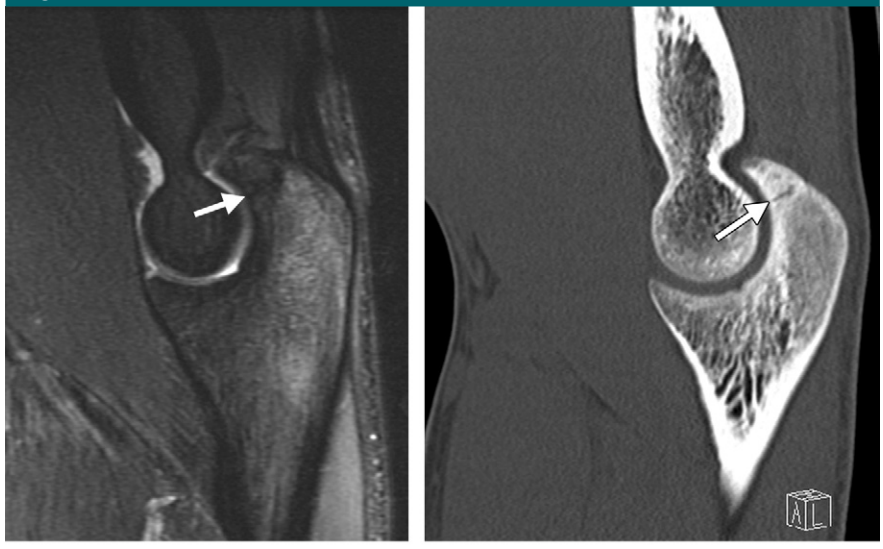

a. b.

Figure 21: **(a)** Sagittal T2-weighted FS MR image of the elbow in a 21-year-old varsity baseball player with a 3-week history of posteromedial elbow pain depicts a low-signal-intensity line through the olecranon tip (arrow) with bone marrow edema throughout the olecranon, compatible with a stress fracture. **(b)** Sagittal reconstructed CT image 1 month later clearly demonstrates the fracture line (arrow).

Humeroradial Plica Syndrome

Plicae are prominent synovial folds of the joint capsule, which are usually asymptomatic. Similar to the knee, synovial folds in the elbow can thicken, in some cases leading to chronic pain and mechanical symptoms. Symptomatic plicae are seen most frequently within the lateral and posterosuperior elbow, insinuating between the radiocapitellar joint (79). Young adult athletes tend to be most frequently affected, particularly those involved in sports requiring repetitive flexion-extension, such as tennis and golf, which can facilitate painful snapping or catching of a thickened synovial fold (80). On MR images, plicae are seen as low-signal-intensity bands outlined by synovial fluid or intraarticular contrast material (Fig 17). A cutoff of 3 mm thickness or greater than one-third coverage of the radial head can be used to accurately suggest the diagnosis of humeroradial plica syndrome (72,81). Associated chondromalacia is frequently seen involving the anterolateral aspect of the radial head (82,83). Focal posterolateral synovitis can also be seen.

Other Nerve Entrapments

Median Nerve

Median nerve entrapment syndromes occur in throwing athletes, although less frequently than ulnar nerve disease. Two common patterns of compression are described (84–86). Pronator syndrome is the most common and arises from compression between the humeral (superficial) and ulnar (deep) heads of the pronator teres muscles secondary to fibrous bands, as the median nerve exits the antecubital fossa. In throwing athletes, the pronator teres may be hypertrophied, contributing to compression with pronation and extension (87,88) Anterior interosseous nerve syndrome (Kiloh-Nevin syndrome) occurs with selective entrapment of this motor branch of the median nerve. Lesions are typically distal to those in patients with pronator syndrome. On MR images, the median nerve can be difficult to see within the elbow because of a lack of perifascial fat and may even appear normal in patients with entrapment; specific compressive lesions are seldom identified (84,86). Occasionally, perineural soft-tissue thickening or signal abnormalities may be seen. Evaluation of the muscle denervation pattern is often the most useful finding with abnormally increased signal on T1- and T2-weighted images within the affected muscles (Fig 22). In pronator syndrome, the affected muscles are the pronator teres, flexor carpi radialis, palmaris longus, and flexor digitorum superficialis, along with muscles innervated by the anterior interosseous nerve. In the more distal anterior interosseous nerve syndrome, the pronator quadratus muscle is always involved, followed by the flexor digitorum profundus muscle, and then the flexor pollicis longus muscle (89). Because the imaging diagnosis often relies on surrogate changes in denervated muscles, MR imaging is variably sensitive for the diagnosis of nerve compression.

Radial Nerve

Radial nerve injury at the elbow is uncommon but can be seen in athletes as a result of overuse. Compression occurs most commonly within the radial tunnel, at the proximal margin of the supinator muscle. The nerve gives superficial (sensory) and deep (motor) branches at this level. The posterior interosseous nerve is the deep motor branch and is vulnerable to compression. At MR imaging, the radial nerve is seen as a low-signal-intensity structure on axial T1-weighted images between the brachialis and brachioradialis before traversing the supinator more distally. As with the median nerve, while a specific site of compression is often difficult to identify, the muscle denervation pattern on MR images is key in making the diagnosis and identifying the compressive level (Fig 23).

Figure 22

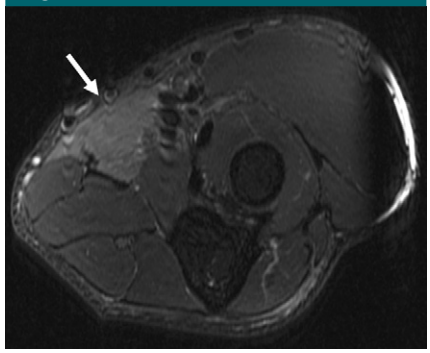

Figure 22: Axial T2-weighted FS MR image in a 46-year-old man with chronic forearm pain demonstrates subtle increased signal intensity within the pronator teres and flexor carpi radialis muscles (arrow) compatible with denervation of the median nerve.

Figure 23

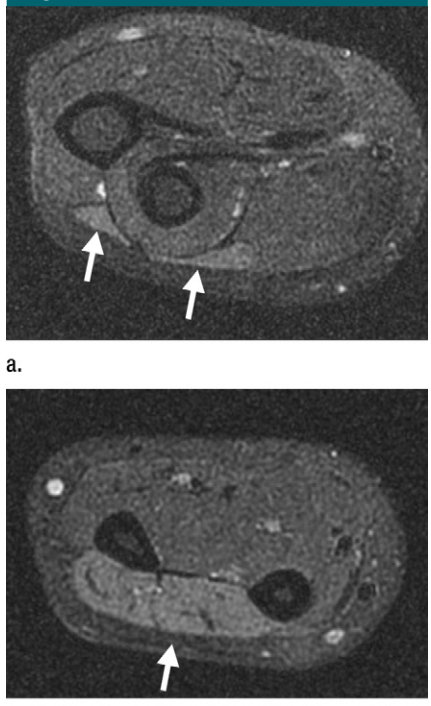

a.

b.

Figure 23: Axial T2-weighted FS MR images in a 16-year-old female patient with left arm posterior interosseous nerve palsy with electromyography findings at the Arcade of Froshe. Images (**a**, more proximal forearm; **b**, more distal forearm) demonstrate increased signal intensity in the extensor compartment musculature (arrows).

Summary

Elbow pain is a frequent presenting symptom in athletes, particularly athletes who throw, occurring as a result of overuse or direct trauma. Standard radiographs can be used to identify fractures or dislocation in the acute setting and can also be used to detail unique patterns of disease secondary to chronic overuse. US allows for targeted soft-tissue evaluation immediately following injury. However, MR imaging is the recommended study of choice for comprehensive evaluation of acute and chronic injuries. Many injuries of the elbow present with overlapping symptoms and prompt imaging evaluation helps to confirm the correct diagnosis and facilitate appropriate treatment.

Disclosures of Conflicts of Interest: M.D.B. disclosed no relevant relationships. **K.J.S.** disclosed no relevant relationships. **L.S.S.** disclosed no relevant relationships.

References

1. Morrey BF, Sanchez-Sotelo J. The elbow and its disorders. 4th ed. Philadelphia, Pa: Saunders Elsevier, 2009.
2. Gregory B, Nyland J. Medial elbow injury in young throwing athletes. Muscles Ligaments Tendons J 2013;3(2):91–100.
3. Munshi M, Pretterklieber ML, Chung CB, et al. Anterior bundle of ulnar collateral ligament: evaluation of anatomic relationships by using MR imaging, MR arthrography, and gross anatomic and histologic analysis. Radiology 2004;231(3):797–803.
4. Cain EL Jr, Dugas JR, Wolf RS, Andrews JR. Elbow injuries in throwing athletes: a current concepts review. Am J Sports Med 2003;31(4):621–635.

5. Mirowitz SA, London SL. Ulnar collateral ligament injury in baseball pitchers: MR imaging evaluation. Radiology 1992;185(2):573–576.
6. Fowler KA, Chung CB. Normal MR imaging anatomy of the elbow. Radiol Clin North Am 2006;44(4):553–567, viii.
7. Fleisig GS, Andrews JR, Dillman CJ, Escamilla RF. Kinetics of baseball pitching with implications about injury mechanisms. Am J Sports Med 1995;23(2):233–239.
8. O'Holleran JD, Altchek DW. The thrower's elbow: arthroscopic treatment of valgus extension overload syndrome. HSS J 2006;2(1):83–93.
9. Salvo JP, Rizio L 3rd, Zvijac JE, Uribe JW, Hechtman KS. Avulsion fracture of the ulnar sublime tubercle in overhead throwing athletes. Am J Sports Med 2002;30(3):426–431.
10. Azar FM, Andrews JR, Wilk KE, Groh D. Operative treatment of ulnar collateral ligament injuries of the elbow in athletes. Am J Sports Med 2000;28(1):16–23.
11. Schwartz ML, al-Zahrani S, Morwessel RM, Andrews JR. Ulnar collateral ligament injury in the throwing athlete: evaluation with saline-enhanced MR arthrography. Radiology 1995;197(1):297–299.
12. Tagliafico AS, Bignotti B, Martinoli C. Elbow US: anatomy, variants, and scanning technique. Radiology 2015;275(3):636–650.
13. Wenzke DR. MR imaging of the elbow in the injured athlete. Radiol Clin North Am 2013;51(2):195–213.
14. Nakanishi K, Masatomi T, Ochi T, et al. MR arthrography of elbow: evaluation of the ulnar collateral ligament of elbow. Skeletal Radiol 1996;25(7):629–634.
15. Cotten A, Jacobson J, Brossmann J, Hodler J, Trudell D, Resnick D. MR arthrography of the elbow: normal anatomy and diagnostic pitfalls. J Comput Assist Tomogr 1997;21(4):516–522.
16. Waldt S, Bruegel M, Ganter K, et al. Comparison of multislice CT arthrography and MR arthrography for the detection of articular cartilage lesions of the elbow. Eur Radiol 2005;15(4):784–791.
17. Dubberley JH, Faber KJ, Patterson SD, et al. The detection of loose bodies in the elbow: the value of MRI and CT arthrography. J Bone Joint Surg Br 2005;87(5):684–686.
18. Lohman M, Borrero C, Casagranda B, Rafiee B, Towers J. The posterior transtriceps approach for elbow arthrography: a forgotten technique? Skeletal Radiol 2009;38(5):513–516.
19. Steinbach LS, Palmer WE, Schweitzer ME. Special focus session: MR arthrography. RadioGraphics 2002;22(5):1223–1246.
20. Bethapudi S, Robinson P, Engebretsen L, Budgett R, Vanhegan IS, O'Connor P. Elbow injuries at the London 2012 Summer Olympic Games: demographics and pictorial imaging review. AJR Am J Roentgenol 2013;201(3):535–549.
21. Hassan SE, Parks BG, Douoguih WA, Osbahr DC. Effect of distal ulnar collateral ligament tear pattern on contact forces and valgus stability in the posteromedial compartment of the elbow. Am J Sports Med 2015;43(2):447–452.
22. Timmerman LA, Schwartz ML, Andrews JR. Preoperative evaluation of the ulnar collateral ligament by magnetic resonance imaging and computed tomography arthrography: evaluation in 25 baseball players with surgical confirmation. Am J Sports Med 1994;22(1):26–31; discussion 32.
23. Del Grande F, Aro M, Farahani SJ, Wilckens J, Cosgarea A, Carrino JA. Three-Tesla MR imaging of the elbow in non-symptomatic professional baseball pitchers. Skeletal Radiol 2015;44(1):115–123.
24. Finlay K, Ferri M, Friedman L. Ultrasound of the elbow. Skeletal Radiol 2004;33(2):63–79.
25. Stevens KJ. Magnetic resonance imaging of the elbow. J Magn Reson Imaging 2010;31(5):1036–1053.
26. Jobe FW, Stark H, Lombardo SJ. Reconstruction of the ulnar collateral ligament in athletes. J Bone Joint Surg Am 1986;68(8):1158–1163.
27. David TS. Medial elbow pain in the throwing athlete. Orthopedics 2003;26(1):94–103; quiz 104–105.
28. Chung CB, Steinbach LS. MRI of the upper extremity. Philadelphia, Pa: Lippincott Williams & Wilkins, 2009.
29. Wear SA, Thornton DD, Schwartz ML, Weissmann RC 3rd, Cain EL, Andrews JR. MRI of the reconstructed ulnar collateral ligament. AJR Am J Roentgenol 2011;197(5):1198–1204.
30. Schwartz ML, Thornton DD, Larrison MC, et al. Avulsion of the medial epicondyle after ulnar collateral ligament reconstruction: imaging of a rare throwing injury. AJR Am J Roentgenol 2008;190(3):595–598.
31. Cohen SB, Valko C, Zoga A, Dodson CC, Ciccotti MG. Posteromedial elbow impingement: magnetic resonance imaging findings in overhead throwing athletes and results of arthroscopic treatment. Arthroscopy 2011;27(10):1364–1370.
32. Loftice J, Fleisig GS, Zheng N, Andrews JR. Biomechanics of the elbow in sports. Clin Sports Med 2004;23(4):519–530, vii–viii.
33. Vitale MA, Ahmad CS. The outcome of elbow ulnar collateral ligament reconstruction in overhead athletes: a systematic review. Am J Sports Med 2008;36(6):1193–1205.
34. Furushima K, Itoh Y, Iwabu S, Yamamoto Y, Koga R, Shimizu M. Classification of olecranon stress fractures in baseball players. Am J Sports Med 2014;42(6):1343–1351.
35. Kooima CL, Anderson K, Craig JV, Teeter DM, van Holsbeeck M. Evidence of subclinical medial collateral ligament injury and posteromedial impingement in professional baseball players. Am J Sports Med 2004;32(7):1602–1606.
36. Sisto DJ, Jobe FW, Moynes DR, Antonelli DJ. An electromyographic analysis of the elbow in pitching. Am J Sports Med 1987;15(3):260–263.
37. Hang DW, Chao CM, Hang YS. A clinical and roentgenographic study of Little League elbow. Am J Sports Med 2004;32(1):79–84.
38. Dellon AL. Musculotendinous variations about the medial humeral epicondyle. J Hand Surg [Br] 1986;11(2):175–181.
39. Husarik DB, Saupe N, Pfirrmann CW, Jost B, Hodler J, Zanetti M. Elbow nerves: MR findings in 60 asymptomatic subject—normal anatomy, variants, and pitfalls. Radiology 2009;252(1):148–156.
40. Gabel GT, Morrey BF. Operative treatment of medical epicondylitis: influence of concomitant ulnar neuropathy at the elbow. J Bone Joint Surg Am 1995;77(7):1065–1069.
41. Bladt L, Vankan Y, Demeyere A, Perdieus D. Bilateral ulnar nerve compression by anconeus epitrochlearis muscle. JBR-BTR 2009;92(2):120.
42. Dahners LE, Wood FM. Anconeus epitrochlearis, a rare cause of cubital tunnel syndrome: a case report. J Hand Surg Am 1984;9(4):579–580.
43. Keen NN, Chin CT, Engstrom JW, Saloner D, Steinbach LS. Diagnosing ulnar neuropathy at the elbow using magnetic resonance neurography. Skeletal Radiol 2012;41(4):401–407.
44. Asamoto S, Böker DK, Jödicke A. Surgical treatment for ulnar nerve entrapment at the elbow. Neurol Med Chir (Tokyo) 2005;45(5):240–244; discussion 244–245.
45. Society of Skeletal Radiology. Low insertion of the medial head of triceps muscle at the elbow. Miami Beach, Fla: Society of Skeletal Radiology, 2012.
46. Baker CLJ, Planscher KD. Operative treatment of elbow injuries. New York, NY: Springer Science & Business Media, 2006.
47. Bartels RH, Verhagen WI, van der Wilt GJ, Meulstee J, van Rossum LG, Grotenhuis JA. Prospective randomized controlled study comparing simple decompression versus an-

terior subcutaneous transposition for idiopathic neuropathy of the ulnar nerve at the elbow: Part 1. Neurosurgery 2005;56(3):522–530; discussion 522–530.

48. Nabhan A, Ahlhelm F, Kelm J, Reith W, Schwerdtfeger K, Steudel WI. Simple decompression or subcutaneous anterior transposition of the ulnar nerve for cubital tunnel syndrome. J Hand Surg [Br] 2005;30(5):521–524.
49. Johnson DH, Pedowitz RA. Practical orthopaedic sports medicine and arthroscopy. Philadelphia, Pa: Lippincott Williams & Wilkins, 2007.
50. Safran MR. Ulnar collateral ligament injury in the overhead athlete: diagnosis and treatment. Clin Sports Med 2004;23(4):643–663, x.
51. Kijowski R, De Smet AA. Radiography of the elbow for evaluation of patients with osteochondritis dissecans of the capitellum. Skeletal Radiol 2005;34(5):266–271.
52. Kijowski R, De Smet AA. MRI findings of osteochondritis dissecans of the capitellum with surgical correlation. AJR Am J Roentgenol 2005;185(6):1453–1459.
53. Rosenberg ZS, Beltran J, Cheung YY. Pseudodefect of the capitellum: potential MR imaging pitfall. Radiology 1994;191(3):821–823.
54. Kobayashi K, Burton KJ, Rodner C, Smith B, Caputo AE. Lateral compression injuries in the pediatric elbow: Panner's disease and osteochondritis dissecans of the capitellum. J Am Acad Orthop Surg 2004;12(4):246–254.
55. Nirschl RP, Ashman ES. Elbow tendinopathy: tennis elbow. Clin Sports Med 2003;22(4):813–836.
56. Potter HG, Hannafin JA, Morwessel RM, DiCarlo EF, O'Brien SJ, Altchek DW. Lateral epicondylitis: correlation of MR imaging, surgical, and histopathologic findings. Radiology 1995;196(1):43–46.
57. Hume PA, Reid D, Edwards T. Epicondylar injury in sport: epidemiology, type, mechanisms, assessment, management and prevention. Sports Med 2006;36(2):151–170.
58. Miller TT, Shapiro MA, Schultz E, Kalish PE. Comparison of sonography and MRI for diagnosing epicondylitis. J Clin Ultrasound 2002;30(4):193–202.
59. Plancher KD, Halbrecht J, Lourie GM. Medial and lateral epicondylitis in the athlete. Clin Sports Med 1996;15(2):283–305.
60. Murphy KP, Giuliani JR, Freedman BA. Management of lateral epicondylitis in the athlete. Oper Tech Sports Med 2006;14(2):67–74.
61. Smith J, Finnoff JT, O'Driscoll SW, Lai JK. Sonographic evaluation of the distal biceps tendon using a medial approach: the pronator window. J Ultrasound Med 2010;29(5):861–865.
62. Athwal GS, McGill RJ, Rispoli DM. Isolated avulsion of the medial head of the triceps tendon: an anatomic study and arthroscopic repair in 2 cases. Arthroscopy 2009;25(9):983–988.
63. Stannard JP, Bucknell AL. Rupture of the triceps tendon associated with steroid injections. Am J Sports Med 1993;21(3):482–485.
64. Sierra RJ, Weiss NG, Shrader MW, Steinmann SP. Acute triceps ruptures: case report and retrospective chart review. J Shoulder Elbow Surg 2006;15(1):130–134.
65. Madsen M, Marx RG, Millett PJ, Rodeo SA, Sperling JW, Warren RF. Surgical anatomy of the triceps brachii tendon: anatomical study and clinical correlation. Am J Sports Med 2006;34(11):1839–1843.
66. Charalambous CP, Stanley JK. Posterolateral rotatory instability of the elbow. J Bone Joint Surg Br 2008;90(3):272–279.
67. Belentani C, Pastore D, Wangwinyuvirat M, et al. Triceps brachii tendon: anatomic-MR imaging study in cadavers with histologic correlation. Skeletal Radiol 2009;38(2):171–175.
68. O'Driscoll SW, Jupiter JB, King GJ, Hotchkiss RN, Morrey BF. The unstable elbow. Instr Course Lect 2001;50:89–102.
69. Potter HG, Weiland AJ, Schatz JA, Paletta GA, Hotchkiss RN. Posterolateral rotatory instability of the elbow: usefulness of MR imaging in diagnosis. Radiology 1997;204(1):185–189.
70. Bredella MA, Tirman PF, Fritz RC, Feller JF, Wischer TK, Genant HK. MR imaging findings of lateral ulnar collateral ligament abnormalities in patients with lateral epicondylitis. AJR Am J Roentgenol 1999;173(5):1379–1382.
71. Ring D, Jupiter JB. Fracture-dislocation of the elbow. J Bone Joint Surg Am 1998;80(4):566–580.
72. Husarik DB, Saupe N, Pfirrmann CW, Jost B, Hodler J, Zanetti M. Ligaments and plicae of the elbow: normal MR imaging variability in 60 asymptomatic subjects. Radiology 2010;257(1):185–194.
73. Tashjian RZ, Katarincic JA. Complex elbow instability. J Am Acad Orthop Surg 2006;14(5):278–286.
74. Hackl M, Wegmann K, Ries C, Leschinger T, Burkhart KJ, Müller LP. Reliability of magnetic resonance imaging signs of posterolateral rotatory instability of the elbow. J Hand Surg Am 2015;40(7):1428–1433.
75. Ahmad CS, ElAttrache NS. Valgus extension overload syndrome and stress injury of the olecranon. Clin Sports Med 2004;23(4):665–676, x.
76. Suzuki K, Minami A, Suenaga N, Kondoh M. Oblique stress fracture of the olecranon in baseball pitchers. J Shoulder Elbow Surg 1997;6(5):491–494.
77. Schickendantz MS, Ho CP, Koh J. Stress injury of the proximal ulna in professional baseball players. Am J Sports Med 2002;30(5):737–741.
78. Chang EY, Fronek J, Chung CB. Medial supracondylar stress fracture in an adolescent pitcher/. Skeletal Radiol 2014;43(1):85–88.
79. Awaya H, Schweitzer ME, Feng SA, et al. Elbow synovial fold syndrome: MR imaging findings. AJR Am J Roentgenol 2001;177(6):1377–1381.
80. Antuna SA, O'Driscoll SW. Snapping plicae associated with radiocapitellar chondromalacia. Arthroscopy 2001;17(5):491–495.
81. Ruiz de Luzuriaga BC, Helms CA, Kosinski AS, Vinson EN. Elbow MR imaging findings in patients with synovial fringe syndrome. Skeletal Radiol 2013;42(5):675–680.
82. McFarland EG, Gill HS, Laporte DM, Streiff M. Miscellaneous conditions about the elbow in athletes. Clin Sports Med 2004;23(4):743–763, xi–xii.
83. Steinert AF, Goebel S, Rucker A, Barthel T. Snapping elbow caused by hypertrophic synovial plica in the radiohumeral joint: a report of three cases and review of literature. Arch Orthop Trauma Surg 2010;130(3):347–351.
84. Bashir WA, Connell DA. Imaging of entrapment and compressive neuropathies. Semin Musculoskelet Radiol 2008;12(2):170–181.
85. Tsai P, Steinberg DR. Median and radial nerve compression about the elbow. Instr Course Lect 2008;57:177–185.
86. Rosenberg ZS, Beltran J, Cheung YY, Ro SY, Green SM, Lenzo SR. The elbow: MR features of nerve disorders. Radiology 1993;188(1):235–240.
87. Konjengbam M, Elangbam J. Radial nerve in the radial tunnel: anatomic sites of entrapment neuropathy. Clin Anat 2004;17(1):21–25.
88. Keefe DT, Lintner DM. Nerve injuries in the throwing elbow. Clin Sports Med 2004;23(4):723–742, xi.
89. Miller TT, Reinus WR. Nerve entrapment syndromes of the elbow, forearm, and wrist. AJR Am J Roentgenol 2010;195(3):585–594.

and echocardiography within 24 hours of each other and tested it on another cohort who met the same inclusion criteria and found very similar results (1).

The idea behind the nomogram model is to take advantage of unused quantitative and semi-quantitative data generated by CT pulmonary angiography, which had already been performed for the diagnosis of pulmonary embolism, in order to use it as a screening tool that can alert the clinicians to the possible presence of an alternative diagnosis that could explain the patient's symptoms (eg, PH).

Dr Huang and colleagues claim that the biostatistical model used should have been based on DCA (2). DCA is a method for evaluating the benefits of a diagnostic test that incorporates clinical consequences of under- or overtreatment (2,3). This is not applicable to the proposed screening tool for PH, which requires high sensitivity (4).

Following the application of the proposed nomogram, it can be expected that clinicians will refer their patients, who show a probability of having PH, to echocardiography for further evaluation rather than directly decide on treatment based on the nomogram alone. We note that our nomogram should be considered as a primary diagnostic tool only after additional experience with its use in a large cohorts of patients. Currently, our prediction model can serve as a screening tool that may alert the clinicians to the presence of PH after exclusion of pulmonary embolism with CT pulmonary angiography.

Disclosures of Conflicts of Interest: G.A. disclosed no relevant relationships. **S.B.** disclosed no relevant relationships. **Y.T.** disclosed no relevant relationships. **T.Z.** disclosed no relevant relationships.

References

1. Aviram G, Shmueli H, Adam SZ, et al. A nomogram based on CT pulmonary angiography for prediction of pulmonary hypertension in patients without pulmonary embolism. Radiology 2015;277(1):236–246.
2. Fitzgerald M, Saville BR, Lewis RJ. Decision curve analysis. JAMA 2015;313(4):409–410.
3. Vickers AJ, Elkin EB. Decision curve analysis: a novel method for evaluating prediction models. Med Decis Making 2006;26(6):565–574.
4. Fletcher RH, Fletcher SW, Fletcher GS. Clinical epidemiology: the essentials. Baltimore, Md: Lippincott Williams & Wilkins, 2012.

Errata

Originally published in:

Radiology 2015;277(2):497–506
DOI:10.1148/radiol.2015141550

Glioblastoma Multiforme Recurrence: An Exploratory Study of ^{18}F FPPRGD$_2$ PET/CT
Andrei Iagaru, Camila Mosci, Erik Mittra, Greg Zaharchuk, Nancy Fischbein, Griffith Harsh, Gordon Li, Seema Nagpal, Lawrence Recht, Sanjiv Sam Gambhir

Erratum in:

Radiology 2016;280(1):328
DOI:10.1148/radiol.2016164020

Page 498, the second Advance in Knowledge should read as follows: with maximum standardized uptake values of 0.**9**–5.**9** (mean, 2.**6** ± 1.2).

Page 550, second paragraph of "Lesion Detection and Changes in Response to Bevacizumab Therapy", first sentence should read: When recurrent GBM was present (17 lesions in 15 patients), the uptake of ^{18}F FPPRGD$_2$ 60 minutes after injection had an SUV$_{max}$ of 0.**9**–5.**9** (mean, 2.6 ± 1.2) prior to treatment.

Figure 3 caption should read: ^{18}F FPPRGD$_2$ PET image shows a **23.8**% decrease in SUV$_{max}$ 1 week after bevacizumab therapy and a **61.9**% decrease 6 weeks after bevacizumab therapy.

Figure E1 caption should read: ^{18}F FPPRGD$_2$ PET image obtained 1 week after bevacizumab therapy shows a 4.**9**% decrease in maximum standardized uptake value (SUV$_{max}$). Figure E2 caption should read: ^{18}F FPPRGD$_2$ PET image obtained 1 week after bevacizumab therapy shows a 5**8**.8% decrease in SUV$_{max}$.

Table 1, first row of data across (Lesion) should read: **2.1** ± **0.8**, 1.**3** ± 0.**8**, 1.**2** ± 0.**7**, .025, .034, .673.

Table 2, Pretreatment value should be **1.5** for patient 8 and **5.9** for patient 11. For patient 12, Volume (cm^3): Change at 1 Week after Bevacizumab (%) should be **–15.6**, and Change at 6 Weeks after Bevacizumab (%) should be **–21.8**. For patient 14, SUV$_{max}$: Change at 6 Weeks after Bevacizumab (%) should be **–36.0**, and Change from 1 to 6 Weeks after Bevacizumab should be **14.3**.

Originally published in:

Radiology 2016;279(1):12–28
DOI: 10.1148/radiol.2016150501
Elbow Imaging in Sport: Sports Imaging Series
Matthew D. Bucknor, Kathryn J. Stevens, Lynne S. Steinbach

Erratum in:

Radiology 2016;280(1):328
DOI:10.1148/radiol.2016164015

The institutional affiliation for Kathryn J. Stevens should be as follows: **Department of Radiology, Stanford University School of Medicine, Stanford, Calif**.

Originally published in:

Radiology 2016;279(3):827–837
DOI:10.1148/radiol.2016151256

Potential Utility of a Combined Approach with US and MR Arthrography to Image Medial Elbow Pain in Baseball Players
Johannes B. Roedl, Felix M. Gonzalez, Adam C. Zoga, William B. Morrison, Mika T. Nevalainen, Michael G. Ciccotti, Levon N. Nazarian

Erratum in:

Radiology 2016;280(1):328
DOI:10.1148/radiol.2016164016

An early online version of the article erroneously described use of the Telos device to apply valgus stress. This has been corrected to reflect that the manual technique was used in the study.